ARTICLES

Can Nature's Design be Improved Upon? High Strength, Transparent Nacre-Like Nanocomposites with Double Network of Sacrificial Cross Links†

Paul Podsiadlo,‡ Amit K. Kaushik,§ Bong Sup Shim,‡ Ashish Agarwal,‡ Zhiyong Tang,|| Anthony M. Waas,§,⊥ Ellen M. Arruda,§,# and Nicholas A. Kotov*,‡,¶,+

Departments of Chemical Engineering, Mechanical Engineering, Aerospace Engineering, Biomedical Engineering, and Materials Science and Engineering, and Program in Macromolecular Science and Engineering, University of Michigan, Ann Arbor, Michigan 48109, and National Center for Nanoscience and Technology, Beijing 100080, China

Received: February 19, 2008; Revised Manuscript Received: April 20, 2008

The preparation of a high-strength and highly transparent nacre-like nanocomposite via layer-by-layer assembly technique from poly(vinyl alcohol) (PVA) and Na^+-montmorillonite clay nanosheets is reported in this article. We show that a high density of weak bonding interactions between the polymer and the clay particles: hydrogen, dipole−induced dipole, and van der Waals undergoing break-reform deformations, can lead to high strength nanocomposites: $\sigma_{UTS} \sim 150$ MPa and $E' \sim 13$ GPa. Further introduction of ionic bonds into the polymeric matrix creates a double network of sacrificial bonds which dramatically increases the mechanical properties: $\sigma_{UTS} \sim 320$ MPa and $E' \sim 60$ GPa.

Introduction

Natural composites possess exceptional mechanical properties.[1–5] Of these, nacre has been especially recognized for its remarkably high toughness and resilience given its composition of 95% of brittle, inorganic $CaCO_3$ tablets and ∼5% of biopolymers. Nacre is twice as hard and more than 1000 times as tough as its constituent phases.[2,6] Both the "brick-and-mortar" architecture and the sacrificial ionic bonds that can reform after breaking are keys to its mechanical properties.[7,8] These amazing properties have inspired scientists to develop synthetic biomimetic analogs.[9,10] Previously, we have reported preparation of a "nacre-like" nanocomposite (NC) via layer-by-layer (LBL) assembly[11] of poly(diallyldimethylammonium chloride) polycation (PDDA, Figure 1A) and inorganic clay nanosheets of Na^+-montmorillonite (MTM).[12] Ionic cross-links were introduced because of the opposite charges on MTM and PDDA. The structure and mechanical properties of this NC were comparable to those of natural nacre and lamellar bones (ultimate tensile strength, $\sigma_{UTS} = 100 \pm 10$ MPa and tangent stiffness after strain stiffening, $E' = 11 \pm 2$ GPa). Later, we also showed that LBL assembly of MTM with poly(vinyl alcohol) (PVA) results in a NC with record-high mechanical properties.[13] We found that post-assembly cross-linking of PVA with glutaraldehyde (GA) increases mechanical properties to $\sigma_{UTS} = 150 \rightarrow 400$ MPa and $E' = 15 \rightarrow 106$ GPa. Despite the high strength, this cross-linking is covalent, which is not present in nacre, and cannot reform, which revealed itself in the low strain values of the resulting composite.

We have posed a question: Can we improve LBL materials and potentially exceed the nature-made mechanical properties of nacre and bones using just the reformable (ionic and other) cross-links? Additionally, one can also pose a question whether bonds other than ionic can be engaged in a similar break-reform fashion.[7,8] These are important goals from both fundamental and practical points of view. Nanoscale nacres potentially afford achieving these goals because they offer a greater degree of (1) integration of organic/inorganic phases and (2) freedom in molecular design when compared with microscale lamellar materials including a wide choice of polymers.[13–15]

In this article, we demonstrate: (1) nacre-like composite with σ_{UTS} far greater than that of any other nacre mimics prepared until now and 2−3× stronger than natural nacre, and (2) the fact that a manifold of weaker bonds can potentially be engaged in a similar manner as sacrificial ionic bonds.

Experimental Methods

Materials. Polyvinyl alcohol (PVA) with molecular weight of MW ≈ 70 000 and 20 wt % solution of poly(diallyldimethylammonium chloride) (PDDA), MW ≈ 100 000−200 000 were purchased from Sigma-Aldrich (St. Louis, MO) and used as received. Na^+-montmorillonite ("Cloisite Na^+", MTM) powder was purchased from Southern Clay Products (Gonzales, TX). The average size of the platelets is 110 nm as described by the manufacturer. From dynamic light scattering, we can state that the degree of exfoliation is virtually 100% in aqueous dispersions. $FeCl_3$, $CaCl_2$, $AlCl_3$, and $CuCl_2$ salts were obtained from Sigma-Aldrich. The 25 mm × 75 mm microscope glass

† Part of the "Janos H. Fendler Memorial Issue".

* To whom correspondence should be addressed. Phone: (734) 763-8768. Fax: (734) 764-7453. E-mail: kotov@umich.edu.
‡ Departments of Chemical Engineering, University of Michigan.
§ Mechanical Engineering, University of Michigan.
|| National Center for Nanoscience and Technology.
⊥ Aerospace Engineering, University of Michigan.
Program in Macromolecular Science and Engineering, University of Michigan.
¶ Biomedical Engineering, University of Michigan.
+ Materials Science and Engineering, University of Michigan.

10.1021/jp801492n CCC: $40.75
Published on Web 07/01/2008

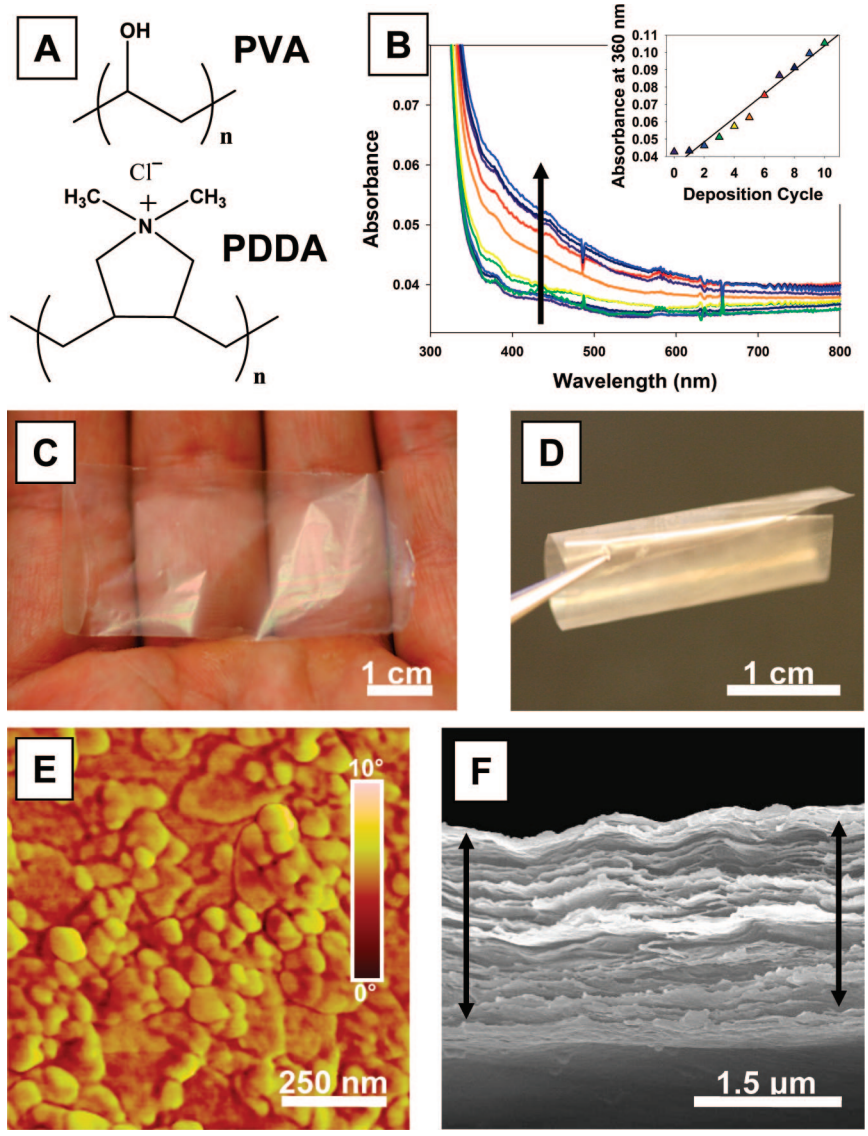

Figure 1. (A) Structure of PVA and PDDA polymers; (B) UV−vis spectra for the first 10 bilayers of deposition (arrow indicates increase of absorbance, inset represents absorbance at 360 nm as a function of bilayer); (C,D) optical images of a free-standing film of $(PVA/MTM)_{300}$ showing very high transparency and flexibility; (E) AFM phase image of a single PVA/MTM bilayer; (F) SEM image of cross section of a 300-bilayer PVA/MTM composite showing laminar architecture. The films in SEM can be slightly expanded due to separation of layers resulting from the shearing force of the razor blade used for cutting test samples.

slides used for the nanocomposites preparation were obtained from Fisher Scientific. Both hydrogen peroxide and concentrated sulfuric acid used in the piranha cleaning solution were purchased from Sigma-Aldrich. Concentrated hydrofluoric acid (HF) was obtained from Sigma-Aldrich, and a 1 vol % HF solution used for preparation of free-standing films was prepared by appropriately diluting the stock solution with DI water. Isopropanol, ACS grade, used in separation of free-standing films was purchased from Sigma-Aldrich. A 0.5 wt % dispersion of MTM, used in the experiments, was prepared by dissolving 5 g of clay in 1 L of 18 $M\Omega \cdot cm^{-1}$, pH = 5.6 deionized water (DI water), under vigorous stirring for 1 week prior to use. After 1 week, insoluble fraction was allowed to sediment, and supernatant was collected. A 1 wt % PVA solution used for LBL assembly was prepared by dissolving 10 g of PVA powder in 1 L of 80 °C DI water under vigorous stirring. The 0.5 M ionic solutions were prepared by dissolving appropriate amounts of salts in DI water. A 0.5 wt % solution of PDDA was prepared by diluting the stock solution with DI water.

Preparation of PVA/MTM Thin Films. Prior to beginning deposition of the PVA-MTM films, the slides were cleaned by immersion into "piranha" solution (3:1 H_2SO_4/H_2O_2, dangerous if contacted with organics) for 1 h, followed by thorough rinsing with DI water. In a typical sample preparation, a clean glass slide was immersed in 1 wt % solution of PVA for 5 min, rinsed with DI water 2 × 1 min and gently dried with compressed air for 1 min, then immersed in 0.5 wt % MTM dispersion for 5 min, rinsed 2 × 1 min, and again dried with compressed air for 1 min. This procedure gave a single deposition cycle and reversal of the surface charge to the original (negative). The cycle could then be repeated as necessary to obtain the desired number of layers. Preparation of the samples was accomplished using a StratoSequence IV, a robotic dipping machine, from nanoStrata Inc. (Tallahassee, FL). After buildup, the glass slides were immersed into the salt solutions for 24 h at room temperature. In the case of Cu^{2+}, the slide was kept in the solution for 3 days. After cross-linking, free-standing films of the composites were isolated with 1 vol % HF solution as described previously.[12] The detached, free-standing films were further dried in a drying oven at 60 °C and then set aside to equilibrate in ambient conditions (~65−75 °F temperature and ~20−30% relative humidity) for at least 24 h prior to

mechanical testing. Films of pure PVA and pure PDDA were prepared by evaporating approximately 65 mL of the 1 wt % and 0.5 wt % solutions of each of the polymers in a 100 mm diameter × 10 mm deep Petri dish in a drying oven at 80 °C for 48 h. PDDA films, because of their hydrophilic nature, were kept dry in the oven until testing.

Instrumental Analysis. LBL process was monitored using an 8453 UV−vis Chem Station spectrophotometer produced by Agilent Technologies. The reference spectrum for the instrument was ambient air, and collected spectra of the adsorbed material were compared to UV−vis absorbance of a fresh, piranha-cleaned glass slide. Atomic force microscopy (AFM) images were obtained using a NanoScope IIIa atomic force microscope (AFM) from Veeco Instruments (Santa Barbara, CA). The instrument was operated in tapping mode with silicon nitride cantilever tips (NSC16/Cr−Au, MikroMasch) at a scan rate of 1 Hz. Ellipsometry measurements were obtained using a BASE-160 spectroscopic ellipsometer produced by J. A. Woollam Co., Inc. The instrument was calibrated to the standard silicon wafer with a thin layer of silicon dioxide, and the subsequent calculations were fitted using Cauchy's model. The samples used for ellipsometry were prepared on silicon wafers following the same LBL protocol described previously. Loading of MTM inside of the free-standing film was determined with a thermo-gravimetric analyzer (TGA) Pyris 1 from PerkinElmer, with a temperature ramp-up rate of 10 °C/min while being purged with air at a flow rate of 20 mL/min. The sample size was chosen between 0.1 and 0.5 mg for all of the samples tested. Scanning electron microscopy (SEM) images were obtained with an FEI Nova Nanolab dual-beam FIB and scanning electron microscope. Because of the nonconductive nature of the specimens, a few nanometers thick layer of gold was sputtered onto the surface of the film prior to imaging. The instrument was operated at 15 kV.

Mechanical Testing of PVA-MTM Films. The tensile mechanical properties were analyzed by two instruments:

(1) Stress−strain curves were obtained by testing ∼1 mm wide and 4−6 mm long rectangular strips of the materials with a mechanical strength tester 100Q from TestResources Inc. (Shakopee, MN). Tests were performed at a rate of 0.01 mm/s with a ∼4.9 N range load cell. The number of tested samples was normally 10−15 for the LBL nanocomposites and 4−5 for the pure polymers. The Young's modulus could not be accurately analyzed with this instrument because of substantial mechanical compliance issues which resulted in inaccurate strain measurements.

(2) The same films (same geometry and batches) were tested in parallel in tension using an in-house designed tensiometer. The tensiometer was built around a Nikon SMZ 800 dissecting microscope that was fitted with a Basler A102 fc digital video camera. Dual actuators were driven by MicroMo stepper motors and mounted on Del-Tron crossed roller slides that enabled the specimen to stay in the center of view. Grips were machined out of stainless steel and placed at the end of both actuators. The specimen ends were adhered to the grips via adhesive tape. The axial servomotors were controlled using LABVIEW software on a Dell Precision 300 personal computer which also synchronized data acquisition from the load element with image acquisition from the digital camera. The samples were loaded at a constant true strain rate of 0.005/sec until failure, and the synchronized force and image recordings were compiled using LABVIEW. Analysis of actual material strain was achieved by electrostatically adhering 25 μm diameter glass beads on the specimen surface. The specimen images were analyzed with LABVIEW software to track the glass bead positions. The raw load versus image data was converted to nominal stress (load/CSA) versus nominal strain data (change in separation of glass beads/initial separation). The Young's modulus was determined by calculating the initial slope of the nominal stress versus nominal strain data. At least five samples were tested in order to produce each data point for the stress−strain curves.

Most of the attributes of the above tensile tests conform to the ASTM standard ASTM D 882. The standard includes the testing of plastic sheets with the thickness not greater than 0.25 mm. The PVA and PVA-MTM samples tested here are within this limit. The standard calls for the measurement of specimen extension by grip extension or displacement of gage marks. Here, the gage marks are the 25 μm diameter glass beads on the specimen surface.

All of the tests were performed under similar environmental conditions with relative humidity maintained in the range of ∼20−30% and ambient temperature in the range of 65−75 °F.

Results and Discussion

As a start, we used LBL films made from PVA and MTM which are bound mainly through a manifold of weak hydrogen bonds. Ionic bonds were introduced after assembly by cross-linking PVA with metal cations M^{n+}.[16−19] Atomic force microscopy (AFM) revealed full platelet coverage of the surface resembling that in nacre (Figure 1E).

Growth profile of the films characterized with UV−vis spectroscopy and ellipsometry (Figure 1B and Figure S1, Supporting Information) revealed fairly linear growth. Ellipsometry measurements gave a thickness of ∼3.5 nm per bilayer for the first 10 deposition cycles. 200- and 300-bilayer films were prepared using an automated dipping machine (nanoStrata Inc., Tallahassee, FL). Once completed, films were cross-linked with 0.5 M solutions of M^{n+}, that is, $FeCl_3$, $CaCl_2$, $AlCl_3$, or $CuCl_2$ for 24 h. Free-standing samples were separated from the slides using a HF etching method described previously[12] and dried at 80 °C for 10 min. Note that, unlike nacre, the ionic bonds in the case of M^{n+} cross-linking are intramolecular with respect to PVA chains rather than between the polymer and the inorganic plates.

The resulting films were found to be strong, flexible, but also highly transparent, which is attributed to the nanoscale dimensions of the inorganic phase (Figure 1C,D) and high orientation of MTM. Light transmittance measurements showed between 50−90% of transparency across the visible spectrum of light for the composites while for plain PVA films it was found to be 90−95% (Figure 2). These results are quite interesting considering that these films are composed of ∼50 vol % (∼70 wt %) clay as was established by thermo-gravimetric analysis (Figure 3). Additionally, the transmittance spectra showed Fabry−Perot fringes which are indicative of high uniformity of the films.[20,21]

SEM revealed a high degree of MTM ordering into a well-defined lamellar structure. (Figure 1F and Figure S2, Supporting Information). The thicknesses of the 200- and 300-bilayer films were found from SEM to be 1.0 μm ± 0.1 μm and 1.5 μm ± 0.1 μm, respectively, which gives ∼5 nm per bilayer when averaged over the entire thickness of the composite. High transparency of the film also allowed for verification of the thickness with ellipsometry; for the 300-bilayer sample, the thickness was nearly identical to that found via SEM: 1.48 μm ± 0.004 μm.

Although no ionic bonds were involved in PVA/MTM bonding, the noncross-linked films actually showed 50%

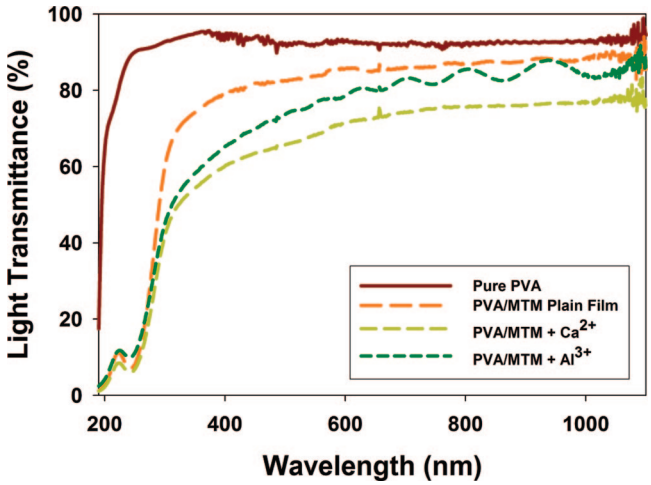

Figure 2. Comparison of UV−vis transmittances for selected $(PVA/MTM)_{300}$ films and pure PVA film.

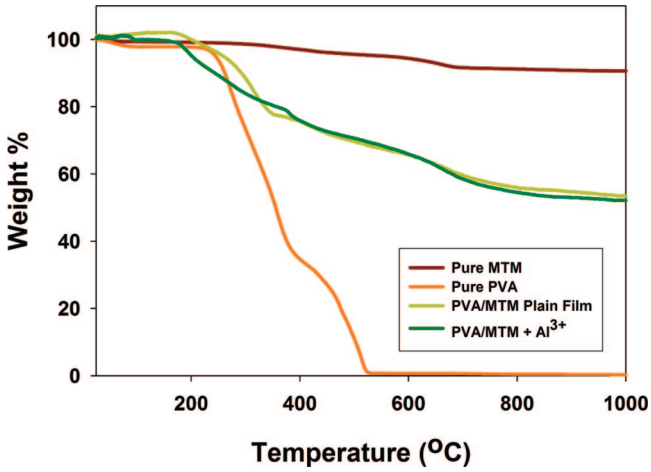

Figure 3. TGA results for PVA/MTM composite with and without Al^{3+} cross-linking, pure MTM powder, and pure PVA.

TABLE 1: Compilation of Mechanical Properties for PDDA/MTM and PVA-Based Composites

	ultimate tensile strength, σ_{UTS} (MPa)	modulus, E' (GPa)	ultimate strain, ϵ (%)
pure PDDA[a]	12 ± 4	0.2 ± 0.03	48 ± 9
pure PVA[a]	40 ± 4	1.7 ± 0.2	35 ± 4
PDDA/MTM	100 ± 10	11 ± 2	10 ± 1
PVA/MTM film	150 ± 40	13 ± 2	0.7 ± 0.2
PVA/MTM + Al^{3+}	250 ± 50	41 ± 5	0.33 ± 0.15
PVA/MTM + Cu^{2+}	320 ± 40	58 ± 6	0.28 ± 0.02

[a] Supporting Information.

higher strength than PDDA/MTM samples studied previously (Table 1).[12,13]

We believe that this increase is due to an abundance of hydrogen and van der Waals bonds that can break and reform when the polymer and clay phases slide against each other similarly to ionic bonds in nacre. They also demonstrated relatively high strains (Figure 4).

The presence of a break-reform mechanism in PVA/MTM can also be seen in the differential strain curve (Figure 4, inset) with a characteristic saw-tooth pattern typical for nacre proteins.[7,8] Implementation of M^{n+} cross-linking showed dramatic increases in tensile strength and stiffness: σ_{UTS}, ~150 MPa → ~320 MPa and E', ~13 GPa → ~60 GPa (arrow indicates change after

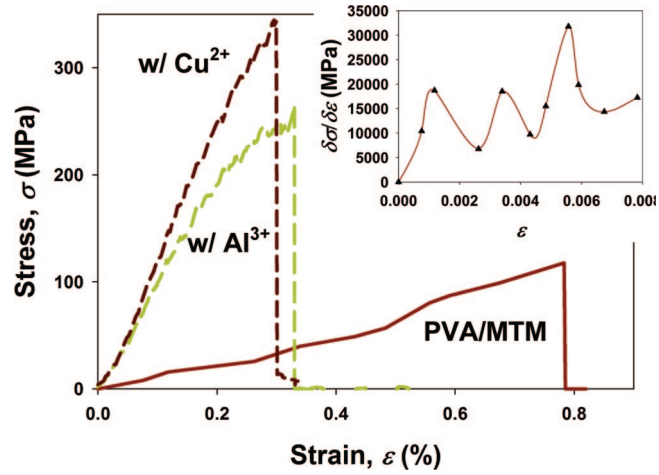

Figure 4. Comparison of stress−strain curves for PVA/MTM films with indicated cross-linkers. Inset shows the differential of the PVA/MTM stress−strain curve revealing the characteristic saw-tooth pattern.

ionic cross-linking). This is especially evident for Cu^{2+} and Al^{3+} treated samples. Ca^{2+} and Fe^{3+}, while being good cross-linking agents for PVA, did not show any improvement at all, which may be attributed to partial bonding of OH groups with clay. The tensile strength of Cu^{2+} cross-linked film is more than twice as high as that of nacre ($\sigma_{UTS} \approx 80-135$ MPa),[4,22] which represents a substantial improvement, and 3× greater than that of the PDDA/MTM composite. Similarly, the stiffness of the Cu^{2+} cross-linked film approaches that of nacre ($E \approx 60-70$ GPa), and it exceeds that of the PDDA/MTM composite by 5 times. Strain, however, remains similar to that seen in the PVA/MTM composites cross-linked by GA. It is also somewhat lower than that of nacre (0.8%),[22] which remains the next materials design challenge but can also be potentially improved upon using appropriate polymers.

Conclusions

We showed here preparation of a thin film of nacre-like clay nanocomposite which utilizes cross-links from both ionic and other weaker bonds. These cross-links are likely to break and form again in the course of the deformation, which can explain several experimental observations. Nevertheless, we need to be cautious and point out that the exact mechanism of the stretching of PVA molecules sandwiched between the parallel sheets on clay will require special study probably by spectroscopic means. Overall, we obtained a material which has superior properties to the original prototype found in nature. This underscores the importance of molecular engineering of the composites and the necessity of the high degree of control over their nanoscale organization. Further directions of improvement of the mechanical performance of these materials must include control over the coiling of the polymer phase to increase extensibility of the material.

Acknowledgment. P.P. thanks the Fannie and John Hertz Foundation for support of his research through a graduate fellowship. We thank J. Lahann and Y. Elkasabi for help with ellipsometry measurements. We thank the Air Force Office of Scientific Research program on multifunctional materials (Grant FA9550-05-1-043) and the U.S. Office of Naval Research (Grant N00014-06-1-0473) for financial support. In memory of Professor Janos H. Fendler, one of the pioneers of biomimetic materials.

Supporting Information Available: Ellipsometry results for initial LBL deposition, additional SEM images of the composite's cross section, and typical stress−strain response curves for pure PVA and PDDA polymers. This material is available free of charge via the Internet at http://pubs.org.

References and Notes

(1) Coyne, K. J.; Qin, X. X.; Waite, J. H. *Science* **1997**, *277* (5333), 1830.
(2) Currey, J. D. *J. Biomech.* **1979**, *12* (4), 313.
(3) Currey, J. D. *Sym. Soc. Exp. Biol.* **1980**, *34*, 75.
(4) Wang, R. Z.; Suo, Z.; Evans, A. G.; Yao, N.; Aksay, I. A. *J. Mater. Res.* **2001**, *16* (9), 2485.
(5) Heslot, H. *Biochimie* **1998**, *80* (1), 19.
(6) Jackson, A. P.; Vincent, J. F. V.; Turner, R. M. *Proc. R. Soc. London, Ser. B* **1988**, *234* (1277), 415.
(7) Smith, B. L.; Schaffer, T. E.; Viani, M.; Thompson, J. B.; Frederick, N. A.; Kind, J.; Belcher, A.; Stucky, G. D.; Mors, D. E.; Hansma, P. K. *Nature* **1999**, *399* (6738), 761.
(8) Thompson, J. B.; Kindt, J. H.; Drake, B.; Hansma, H. G.; Morse, D. E.; Hansma, P. K. *Nature* **2001**, *414* (6865), 773.
(9) Sellinger, A.; Weiss, P. M.; Anh, N.; Lu, Y.; Assink, R. A.; Gong, W.; Brinker, C. J. *Nature* **1998**, *394* (6690), 256.
(10) Deville, S.; Saiz, E.; Nalla, R. K.; Tomsia, A. P. *Science* **2006**, *311* (5760), 515.
(11) Decher, G. *Science* **1997**, *277* (5330), 1232.
(12) Tang, Z.; Kotov, N. A.; Magonov, S.; Ozturk, B. *Nat. Mater.* **2003**, *2* (6), 413.
(13) Podsiadlo, P.; Kaushik, A. K.; Arruda, E. M.; Waas, A. M.; Shim, B. S.; Xu, J.; Nandivada, H.; Pumplin, B. G.; Lahann, J.; Ramamoorthy, A.; Kotov, N. A. *Science* **2007**, *318* (5847), 80.
(14) Podsiadlo, P.; Tang, Z.; Shim, B. S.; Kotov, N. A. *Nano Lett.* **2007**, *7*, 1224.
(15) Podsiadlo, P.; Liu, Z.; Paterson, D.; Messersmith, P. B.; Kotov, N. A. *Adv. Mater.* **2007**, *19* (7), 949.
(16) Kandori, K.; Ishikawa, T. *Colloid Polym. Sci.* **2004**, *282* (10), 1118.
(17) Bonapasta, A. A.; Buda, F.; Colombet, P. *Chem. Mater.* **2000**, *12* (3), 738.
(18) Bonapasta, A. A.; Buda, F.; Colombet, P.; Guerrini, G. *Chem. Mater.* **2002**, *14* (3), 1016.
(19) Gong, J.; Luo, L.; Yu, S. H.; Qian, H.; Fei, L. *J. Mater. Chem.* **2006**, *16* (1), 101.
(20) Mamedov, A.; Ostrander, J.; Aliev, F.; Kotov, N. A. *Langmuir* **2000**, *16* (8), 3941.
(21) Guan, Y.; Yang, S.; Zhang, Y.; Xu, J.; Han, C. C.; Kotov, N. A. *J. Phys. Chem. B* **2006**, *110* (27), 13484.
(22) Barthelat, F.; Li, C. M.; Comi, C.; Espinosa, H. D. J. Mater. Res. . **2006**, *21* (8), 1977.

JP801492N